X-15070 [redacted]

C.T

001723 NMC-AER-6C

NEW MEXICO COLLEGE
OF AGRICULTURE AND MECHANIC ARTS

PHYSICAL SCIENCE LABORATORY

STATE COLLEGE, NEW MEXICO

NMC-AER-6C
SCDC-3089X
X-15070
C.T

ADJACENT TO AND COOPERATING WITH
WHITE SANDS PROVING GROUND

UNCLASSIFIED

TELEPHONE
LAS CRUCES 800

SANDIA SYSTEMATIC DECLASSIFICATION REVIEW	
1st Review Date 10-21-96	Determination (Circle Number):
Authority: ☐ ADC ☒ ADD	1) Classification Retained
Name: W. Layne	2) Classification Changed to: U
2nd Review Date 10/30/96	3) Contains No DOE Classified Information
Authority: ADD	4) Coordinate With
Name: R. T. Duff	5) Classified UCAR
	Comment: NO UCAR

SC DC-3089X

AER-6C

001723

A General Discussion of the
Reduction and Analysis Procedure
used on Flight Series #2

SANDIA SYSTEMATIC DECLASSIFICATION REVIEW	
[illegible] DECLASSIFICATION STAMP	
U	R. T. Duff
Emelda Selph 11-25-96	RECORD ID 97SN096
W C Layne 11-26-96	DATED 10/30/96
[illegible] & DATE	

P.O. No. EL-5[illegible]

17 July 1953

[redacted]

Distribution:
Copy 1 - R. H. Moore, Sandia Corp.
Copy 2 - ~~[illegible]~~, Sandia Corp. T. S. Church
Copies 3, 4 - Classified Documents File, Sandia Corp
Copies 5, 6 - ABL File, PSL, NMA&MA

TECHNICAL REPORT SECTION
SANDIA CORPORATION
[redacted]

UNCLASSIFIED

1156/24

[redacted]

UNCLASSIFIED

TABLE OF CONTENTS

Section		Page
I	Introduction	2
II	Log of Flights	3
III	Qualitative Rating of Films	4
IV	Altitude Determination	5
V	Antenna Pattern Approximation	8
VI	Pulse Duration	9
VII	Peak Transmitted Power	10
VIII	Calibration Procedure	11
IX	Preparation of Reading Scales	12
X	Aerial Photo Composites	15
XI	Overlays	19
XII	Film Reading	23
XIII	Estimations of the Probability Density Function	30
XIV	Estimations of the Cumulative Probability Curves	[illegible]
XV	The Distribution $W(R) = \frac{R}{\psi_0} e^{-\frac{R^2+P^2}{2\psi_0}} I_0\{RP/\psi_0\}$	[illegible]
XVI	The Establishment of Confidence Intervals for the Estimation of P_r and $\sqrt{E(R^2)/2}$	[illegible]
XVII	The Establishment of Confidence Intervals for the Cumulative Density Points	[illegible]
XVIII	Determination of the Scattering Coefficient	[illegible]
Figures	1 through 5	

[redacted]

UNCLASSIFIED

I. INTRODUCTION

This is a general report covering the methods of analysis and general background material applicable to all the films of Flight Series 2.

For the results of the reduction and analysis of data from individual films one is referred to individual film reports as follows:

Film No.	Report No.
2-5	AER-6D
2-7	AER-7A
2-21	AER-7D
2-23	AER-7E
2-22	AER-7F
2-9	AER-7G
2-10	AER-7H
2-13	AER-7I
2-1[illegible]	AER-7J
2-13	Not yet assigned
2-14	" " "
2-1[illegible]	" " "

[redacted]

UNCLASSIFIED

II. LOG OF FLIGHT. -

The information supplied with the films of Flight Series 2 is assembled in Figure 1, except for detailed calibration data which is included in a later section which is devoted to calibration procedure.

As will be noted again in a section devoted to altitude determination, omission of radar altitudes from the data made the processing far unusually more difficult and introduced considerable uncertainty into the analysis.

In the analysis of Flight Series 2 no attempt was made to use the altitude indicator which appears in the theater pictures.

[redacted]

UNCLASSIFIED

III. QUALITATIVE RATING OF FILMS

The first step in the data reduction process was to rate the films qualitatively (or semi-quantitatively) based on a preliminary scanning on a Model C Recordak. Of the 23 films in Flight Series 2, 18 were classed as usable and 5 were rejected as unusable. The results of this survey are summarized in Figure 2. Although the return pulse amplitudes in the column headed "Return Range" could be converted to scope deflection in mm, it is perhaps just as useful to consider them only as relative heights; the same applies to the column headed "Comparator Range". It will be noted that the principal rejection cause was failure to have the return pulse bracketed by markers. This is serious because the sweep speed is not constant across the face of scope; it is essential to determine the sweep speed factor for that portion of the sweep which contains the return.

Another serious problem exists when a marker falls somewhere in the return pulse. The usual effect is that it knocks out two reading positions, assuming reading positions corresponding to terminal 5, 10, 15 and 20 degree angles: the trace is completely obscured at one reading position and its appearance at one of the adjacent positions is unreliable.

A third serious problem was caused by the erratic appearance of spurious traces. These were presumed to be due to arcing taking place in a failing converter (the flight series was finally terminated by converter failure). The frequency of occurrence of these spurious traces ranged from less than 1% to as high as about 20%. Even if all spurious traces were recognized they would constitute a serious deficiency. But the situation is made much worse by the fact that often the film readers, not knowing much about what they were looking at, were unable to differentiate between spurious and normal traces. Every effort should be made to eliminate them completely.

Generally the films in Flight Series 2 represented a considerable improvement over those of Flight Series 1 and earlier groups.

It appears that the six films for which the antenna was oriented obliquely (2-6, 2-8, 2-14, 2-17, 2-19, 2-20), although otherwise usable, may prove to be unusable because of questions about the range marker equation which must be used in the reading scale preparation procedure.

Sample film strips from 22 films in Flight Series 2 are attached to this report. Film number 2-1 was returned to Dr. Moore as an example of one rejected because the return was not bracketed by a time-marker.

[redacted]

UNCLASSIFIED

IV. ALTITUDE DETERMINATION

The absolute altitude of the aircraft to be associated with any particular film would ordinarily be taken as that indicated by the SCR-718 radar carried by the plane, and this altitude would be checked by some independent method or methods. However, for Flight Series 4, the SCR-718 radar either was not in the plane or was inoperative, so that no radar altitudes were available.

The first attempt in establishing the aircraft altitude above the terrain for each film was by making use of the pressure altimeter readings which were available in the flight log. We assumed that the altimeter settings had been corrected for local barometric pressure to give altitude above sea level at some standard temperature, and that the recorded pressure altitude could be converted into actual altitude above ground by applying corrections for both temperature and ground altitude. This might seem to be a straightforward method, but the fact is that it is an unsatisfactory one. The altitude of the ground, for instance, had to be determined by reference to the appropriate sectional aeronautical chart, on a basis of contours separated by 500 or 1000 ft. and of a few spot elevations. As a check on the altitudes determined by this method, careful measurements were made of the photo distances between two points which occurred in the several photos taken of a given site and this information was used to order the photographs with respect to altitude. This order did not always agree with that indicated by the recorded pressure altitudes. For these reasons this method of altitude determination was abandoned.

The last test was to infer altitudes from a study of the photographs themselves. From the simple geometry of the optics of the problem

$$h = \frac{d_g}{d_p} f$$

where h = altitude in feet (distance from ground to camera lens)

f = focal length in mm of simple lens equivalent of camera lens system.

d_g = distance in feet between two points on ground

d_p = distance in mm between same two points on photograph.

[redacted]

UNCLASSIFIED

[redacted]

UNCLASSIFIED

Clearly then the altitude is determined if we have

(1) The focal length, f.

(2) Section lines (5280 ft separation) clearly visible on photograph so that the corresponding measurements of d_p could be made.

With respect to the focal length, f, a figure of 306 mm had been quoted by Dr. Moore, Sandia, to Mr. Carbine by phone on 3 March 1953 (this was confirmed in an enclosure to a letter, dated 23 March, from Daly at Sandia). A cursory check at the time had confirmed this figure to be at least approximately correct, and in the determination of altitudes for Flight Series 2 this figure was used.

With respect to the distance between section lines on the photograph, it was desired to determine d_p as the average of as many such independent determinations as could be had from the several photographs in the sequence taken at the particular altitude which was being determined. For this purpose, run 3B of Flight Series 2 was chosen since it involved a large number of photographs (photos 24 through 42, inclusive). Thirteen independent measurements of the one-mile section interval yielded an average d_p value of 140.8 mm. The associated standard deviation was quite small, actually only 0.4 mm or 0.3%.

Using these values of f and d_p, the altitude at which photos 3B were taken was thus established at 11470 feet. This was then taken as a standard and the altitudes of other runs over Site 8 were determined from it by use of the relation

$$h_x = \frac{d_s}{d_x} h_s$$

where d_s and d_x are the distances between the same two definitely identifiable points on photo 3B and photo X respectively. By reference to the earlier equation it is seen that the uncertainty in any altitude in the Site 8 runs is due to the combined effect of the uncertainty in f, plus uncertainties of probably 0.1% in the one-mile section interval on the ground, and about 0.1% in the measured section interval on the photograph. As will be shown later in this report, the uncertainty in f is probably as much as 1.6%, so that the probable uncertainty in the altitudes for Site 8 is not far from 1.5%. This is a sizeable uncertainty, running from 34 feet at an altitude of 4000 feet to 176 feet at an altitude of 11000 ft. This large uncertainty in the Site 8 altitudes is of course, due to the fact that there were not available any radar altitudes which were directly applicable, or which could be used as a standard for reference purposes.

[redacted]

UNCLASSIFIED

[redacted]

With respect to the runs over Site 2, the altitudes were established in a somewhat similar manner, except that this time there was available for use as a standard, a radar altitude associated with the Site 2 (8300 feet associated with GR Film 1-16 of Flight Series 1). Likewise, the altitudes for the runs over Site 6 were based on an altitude of 10840 feet established for GR Film 2-14; this altitude was taken to be the average of 3 independent determinations based on radar altitudes given for 3 different runs in Flight Series 1. For Sites 2 and 6 the uncertainty in the altitudes, by reference to the last equation above, is seen to result from the combined effect of the uncertainties in the distances d_s and d_x on the photographs, plus the uncertainty in the radar altitude taken as a standard.

Taking the uncertainties in the standard altitudes to be approximately 0.6%, and, as before, assuming about 0.1% uncertainty introduced by each of the measurements d_s and d_x, the probable error in the altitudes determined for Sites 2 and 6 is seen to be still approximately 0.6%. This means about 25 feet at an altitude of 4000 feet or 65 feet at 11000 feet.

As mentioned above it was desired to have an independent check of the effective focal length of the K-17 camera for comparison with the figure of 306 mm supplied by Sandia. Clearly, for such an independent check it is sufficient to have photographs

(1) for which radar altitudes are available

and (2) on which section lines are clearly visible.

Of all the photographs for which radar altitudes are available only those of Site 2, Flight Series 1 (Missouri farmland near Kansas City) meet the above requirements. Rearranging the first equation in this section we have

$$f = \frac{d_p}{d_g} \ell$$

Twelve independent determinations, involving measurements from 6 different photographs, yielded as a mean value $f = 311$ mm. Although the standard deviation was not computed, the precision was fairly good, all values falling between the limits 277 and 322. Had 311 mm been used in place of the 306 mm focal length, the altitudes for Site 2 of Flight Series 2 would have been increased by 1.6%.

[redacted]

[redacted]

UNCLASSIFIED

V. ANTENNA PATTERN APPROXIMATION

During the course of the analysis it is necessary to use an analytic approximation to the antenna pattern. The requirement is that this be as simple as possible, and so it was chosen to be Cos 3θ, where θ is the angle from the axis of the antenna and which assumes circular symmetry about this axis and defines the pattern out to an angle of 30°. It may be observed that the half power point of the approximation is located at a beam half angle of 20° and compares favorably with the measured antenna patterns whose half power half angles averaged 18.3°. The measurements also justify the assumption of circular symmetry to a good extent. The actual measured patterns may be seen by reference to report AWR 54.

[redacted]

UNCLASSIFIED

[redacted]

UNCLASSIFIED

VI. PULSE DURATION

Analysis of radar return, as directly applied to the determination of the reflection coefficients, is facilitated by the assumption of a rectangular pulse shape, and therefore requires the choice of some arbitrary pulse duration. Figure 3 shows the transmitted pulse and its rectangular approximation plotted on a linear power scale and against time. As can be seen, the transmitted pulse is not rectangular, but rises gradually to a sloping top and then descends even more gradually. The criterion used in our choice of pulse duration was that of the width of the pulse at the half power points, yielding a pulse duration of .225 microseconds. The approximation is shown such that the area under its curve is equal to the area under the curve of the transmitted pulse and thus illustrates the degree to which the rectangular assumption is justified. It is to be noted, however, that the gradual rise of the leading edge introduces a time delay which greatly influences zone definition, and therefore cannot be neglected in zone analysis, since zone dimensions are a vital factor in the reflection coefficients. Further discussion on the effect of this time delay is given in Section IA of this report.

[redacted]

UNCLASSIFIED

[redacted]

VII. PEAK TRANSMITTED POWER

Average transmitted power measurements were made for each film-run of this flight series by means of a calibrated directional coupler feeding a power bridge. Peak transmitted power may be determined from these measurements by the expression:

$$P_t = \frac{P_{\text{power bridge}} \times \text{Attenuation factor}}{\text{Rep-rate} \times \text{Pulse width}}$$

where the attenuation factor corresponds to the db drop of the directional coupler minus the db drop through the antenna cable system, thus referring the transmitted power to the antenna terminals. The attenuation factor was, therefore, the power ratio corresponding to 38.25 db or 6.68×10^3 and the expression becomes:

$$P_t = \frac{6.68 \times 10^3}{1600 \times .225 \times 10^{-6}} P_{\text{power bridge}} = 1.86 \times 10^7 \times P_{\text{power bridge}}$$

where $P_{\text{power bridge}}$ is given in watts.

[redacted]

[redacted]

VIII. CALIBRATION PROCEDURE

The calibration data supplied was in the form of scope deflections versus signal generator attenuator settings. To facilitate the analysis, these settings must be converted to microvolts and referred to the antenna terminals. This conversion to an absolute scale is dependent upon accurate measurements of gain at several points in the system, and a measurement of the reference power of the signal generator. This latter was accomplished by feeding the signal generator directly into the power bridge which was used as a standard. The former measurements were made preliminary to this flight series, and the relative gain of the comparator signal injection point was found to be 11.29 db above that of the antenna terminals. However, subsequent to this flight series, it was discovered that the gain of the injection point of the comparator signal was a function of frequency, thus introducing an uncertainty in the absolute signal level. This uncertainty, which is due to lack of resetability in frequency, is estimated to be $\pm$ 3 db. It is probable that the frequency does not drift appreciably during the several seconds of any run, and therefore the comparator signal can be considered constant throughout the run. However, the uncertainty still remains between successive runs, since it was during this time that tuning adjustments were made. Some argument, therefore, still remains as to how to treat the data when apparent variations of system gain are indicated from run to run by the different comparator pulse amplitudes observed. The procedure used, almost arbitrarily chosen, was to assume the gain of the comparator signal injection point to be constant. Next, the calibration data was converted to microvolts referred to the antenna terminals, on the basis of the 11.[illegible] db figure and a [illegible] ohm transmission line. These values were plotted (Figures [illegible] and [illegible]), and from these curves the semi-automatic film reader was set up for each scope setting and films were read to yield numbers proportional to microvolts for each series of films using that scope setting. [illegible] thus yielded an average comparator pulse amplitude, which when compared with the amplitude expected on the basis of the signal generator attenuator settings, gave a linear correction factor to be applied to the readings. This factor was lumped in with the reader proportionality factor and applied to the data during the course of the analysis. Effectively the comparator signal was thus used as a reference, and the 11.[illegible] db gain figure was corrected from run to run.

[redacted]

[redacted]

IX. PREPARATION OF READING SCALES

The appearance of a typical trace is shown schematically below.

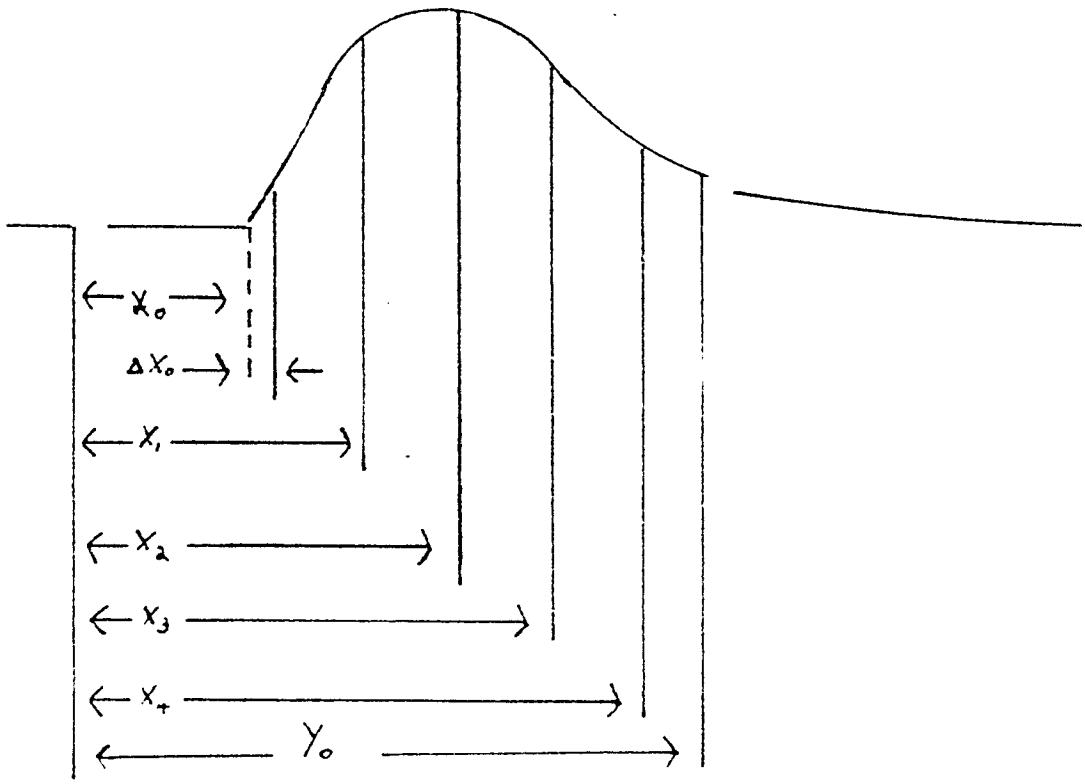

Part of the desired outcome from the data reduction and analysis of each film is the determination of the reflection coefficient of the terrain involved, as a function of the angle between the direction of propagation of the incident radiation and the normal to the terrain. Specifically, it was desired to get reflection coefficients for terrain located at angles of 5, 10, 15 and 20 degrees from the vertical. This was treated briefly in Section C-5 of ANR-6. There it was shown how the proper sampling times, measured from the beginning of the return pulse, could be read

[redacted]

directly from a plot of the family of t-vs-θ curves

$$\tan^2\theta = \frac{c}{h}t + \frac{c^2}{4h^2}t^2$$

where the altitude h is the family parameter. These sampling times are converted into sampling distances from the beginning of the return by multiplication by the sweep speed factor applicable for the film reader magnification being used. These distances from the first return are converted to distances from the beginning of the previous time-marker by adding X_0, the average distance from the beginning of the time-marker to the beginning of the pulse rise. These distances (X_1, X_2, X_3 and X_4) scribed on a transparent plastic sheet indicate the horizontal positions at which readings are taken. The magnitude of the pulse amplitude at any such position is read out by the film reader when the plastic scale is moved vertically till the cross lines intersect the trace and the button is pushed (The PSL Film Reader with lamp bank output was described in AER-6, Section C-2).

A typical reading scale is shown in the above diagram. The first step in producing it was to determine X_0. This was done by averaging the result obtained by two or more readers. Each reader obtained his result by averaging 50 X_0 distances taken at random positions scattered throughout the film. A next step was to determine the sweep speed applicable over the interval containing the return pulse. Again, this was done by averaging the result obtained independently by at least two readers. And, as before, each reader obtained his result as the average of 50% distances.

After the reading times from the beginning of the rise of the return pulse have been determined, it is easy to calculate the outside radii and outside angular positions of the associated illuminated area, by using the equations

$$r^2 = hct + \frac{c^2t^2}{4}$$

and

$$r = h\tan\theta$$

The inner radii and inner angular positions are similarly determined by subtracting the pulse duration, 0.225 μ sec for Flight Series 2, from the above times and computing as before. It is considered to be a satisfactory check on the whole process if the inner angular positions turn out to be as much below the nominal angle as the outer angular position is above it.

[redacted]

The transmitted pulse is, of course, not a rectangular pulse, but has a leading edge which rises gradually. The effect of this gently rising leading edge of the transmitted pulse is to cause the return pulse to begin to rise earlier than it would if the leading edge were steeper. An analysis of this problem will be included in WSR-7. The conclusion is that the effective beginning of the rise, for the transmitted pulse used in Flight Series 2, should occur later by about .0405 μ sec. than the just detectable beginning of the pulse rise. Multiplication by the sweep speed factor for the film yields the correction, ΔX_0 in the diagram above, which should be added to X_0. This correction was made for all films in Flight Series 2 before they were reported, except for films 2-5 and 2-7 for which supplemental reports will be made.

[redacted]

A. AERIAL PHOTO COMPOSITES

The first task was the association unambiguously of the 153 Flight Series 2 aerial photographs with 23 separate runs at various altitudes over 3 sites. This was not easy since it had to be accomplished without benefit of a log. The results were as follows:

Aerial Photo Number	Site Number	Run Number	No. Photos in series	Comment
1-3			3	Note A
4-8	8	1	5	Note B
9-13	8	2	5	
14-18	8	3	5	
19-23	8	3A	5	
24-42	8	3B	19	
43-47	8	4	5	Note C
48-52	8	5	5	
53-56	8	6	4	
57-16	8		5	
62-66	8	7	5	Note D
67-71	8	8	5	
72-76	8	9	5	
77-82	8	10	6	Note E
83-87	8	11	5	
88-91	8	12	4	
92-96	2	13	5	Note F
97-102	6	14	6	
103-107	2	15	5	
108-112	6	16	5	
113-117	2	17	5	
118-122	6	18	5	
123-127	2	19	5	
128-132	6	20	5	
133-137	2		5	
138-142	6	21	5	
143-147	2	22	5	
148-153	6	23	6	

[redacted]

Note A: Photos 1-3 - These were excluded since they could not be associated with any of the Sites 2, 6, and 8.

Note B: Photos 4-42 - Run number assignment is believed to be correct.

Note C: Photos 43-61 - Run number assignment is consistent with the given pressure altitude information (e.g., photos 48-52 were taken at a higher altitude than the others in the group), but either photos 53-56 or 57-61 constitute an extra (unaccounted for) set and it was not possible to determine definitely which to associate with run number 6. In preparing photo composites it was assumed that photos 57-61 actually corresponded to run 6 and that probably photos 53-56 accompanied a pass which for some reason yielded no GR camera data.

Note D: Photos 62-76 - Run number assignment believed to be correct.

Note E: Photos 77-91 - Run number assignment believed to be correct.

Note F: Photos 92-153 - In this group there is an extra set of Site 2 photos and, by working from both ends of the group, this extra set was pinned down to photos 133-137. This conclusion is strengthened by the fact that it preserves the alternating 2-6-2. . . series which would otherwise be broken. The assumption is that no GR camera data was taken to accompany photos 133-137.

Note G: The number of photos taken in each sequence is usually, but not always, 5; a considerable range was noted, from as few as 3 to as many as 19.

Note H: No aerial photo shortage (as had been reported) was found. In fact, in addition to a full complement, there were 3 extra sets which were unaccounted for.

The photo composites themselves were made from the first three photos in each series. Since the scale distortion increases as one proceeds outward from the center of the photograph, adjacent photographs will match up best if the line of overlap is located equidistant from the centers of both photos. This criterion was followed as a general rule, although it had to be deviated from in those cases where by following it there would have been no detail to guide by at the overlap position. Since the radar return data were taken when the aircraft was approximately over the center of the first photo in the series, it was trimmed only as necessary

to match up with the second photo in the series. The second photo was, of course, trimmed on both sides. The third photo usually lay entirely outside the illuminated area, and since its function was only one of rounding out one's visual impression of the sort of terrain involved, it was trimmed as needed to keep the size of the whole photo composite reasonable (i.e., so that when cut in two and hinged with scotch tape it could conveniently be inserted between the pages of an already bound report).

On the composite the center of each photo is indicated. This was easy to do before the original photos were trimmed, by reference to center markers along the photo edges. The line of flight was indicated by a vector roughly averaging the positions of the photo centers. The composites were identified both by GR film number and by report number.

[redacted]

UNCLASSIFIED

XI. OVERLAYS

For use in conjunction with the photo composites it was felt desireable to have also a transparent overlay bearing certain information relating to the particular run. Perhaps most important were the zone boundary circles, drawn to scale for the particular altitude and reading times involved. Also included were the associated zone boundary angles, radii, and relative antenna gains. Finally, there was added the distance travelled by the aircraft in two seconds (which is approximately the time of run of the GR camera). This distance is only approximate, as the aircraft ground speed was usually not known and winds aloft are often comparable in magnitude to the indicated air speed of aircraft in the C-47 class.

The procedure involved in obtaining zone boundary angles and radii was described in the section headed Reading Scale Preparation.

The overlay may, of course, by moved about over the composite according to the judgement of the reader. This freedom is desireable since the position of the aircraft when the GR camera data were taken, with respect to the photo composite, was not well known.

[redacted]

UNCLASSIFIED

[redacted]

UNCLASSIFIED

XII. FILM READING

As a general rule for Flight Series 2, every third trace throughout the usable portion of the film was read. However, for films 2-5, 2-7, and 2-22, first 2500 traces were read consecutively; this was followed by some such scheme as reading every second, every third, or every fifth trace thereafter throughout the remainder of the films. The idea behind the 2500 consecutive traces was to make it possible to make preliminary autocorrelation studies on a few films in Flight Series 2.

Reproducibility checks were run on 200 trace intervals in a couple of films. Qualitatively, the reproducibility was reasonable, about as expected. More will be said about film reading reproducibility in a later report.

[redacted]

UNCLASSIFIED

[redacted]

UNCLASSIFIED

XIII. ESTIMATIONS OF THE PROBABILITY DENSITY FUNCTION

The probability density functions for the return voltages (voltages at antenna terminals) are estimated for each zone and these estimates are plotted together on one large graph in the individual film reports. The probability that a voltage lies in an interval, Δd, is estimated by $\hat{p} = n/N$ where n equals the number of voltages in Δd and N is the total number of voltages sampled. This estimate, $\hat{p}$, is divided by Δd and the quotient is plotted above the midpoint of Δd. This is done so that the area under the curve will give the probability directly. The density function, f(x), is defined by the relationship:

$$\text{Probability} \left\{ a < x < b \right\} = \int_a^b f(x)\, dx$$

With regard to the number of intervals Δd, the following dilemma arises. The more probable the occurrence of a voltage in an interval, the more accurately the probability can be estimated. This would lead us to take a very small number of intervals with, consequently, a high probability attached to each. However, the fewer intervals, the fewer points and consequently the less that can be determined about the shape of the curve. Thus, you must take enough points to determine the shape of the curve, and yet not any more than necessary since the fewer you take the more accurate they are. We relied upon approximately 10 intervals with the highest one being larger than the rest and including all the high, rare voltages together.

[redacted]

UNCLASSIFIED

[redacted]

UNCLASSIFIED

XIV. ESTIMATIONS OF THE CUMULATIVE PROBABILITY CURVES

The cumulative probability curves for the return voltages are estimated for each zone and plotted together on the same set of coordinant axis in the individual film reports. The probability is again estimated by $\hat{p} \doteq n/N$ where n is now the number of voltages less than the upper limit of the interval and N is the total number of voltages sampled. This estimated probability is plotted against the upper limit of the interval. In the individual film reports these estimated cumulative probability curves were also plotted on both Rayleigh and normal paper. Cumulative curves of the form

$$F(x) = \int_0^x t/\psi_0 \; e^{-\frac{t^2}{2\psi_0}} \, dt$$

plot as straight lines on Rayleigh paper while cumulative curves of the form

$$G(x) = \int_{-\infty}^x \frac{1}{\sqrt{2\pi}\,\sigma} \; e^{-\frac{(t-\mu)^2}{2\sigma^2}} \, dt$$

plot as straight lines on normal paper. This was done in hopes that a family fitting the return from all the zones might be discovered.

[redacted]

UNCLASSIFIED

[redacted]

UNCLASSIFIED

XV. THE DISTRIBUTION $W(R) = R/\psi_0 \, e^{-\frac{R^2+P^2}{2\psi_0}} I_0\{RP/\psi_0\}$

In AER-5, Section VII, the distribution W(R) above was derived as a possible outcome for the antenna voltages. If we express the voltage R in units of $\sqrt{\psi_0}$, and let $a = P/\sqrt{\psi_0}$, the distribution of the new variable $x = R/\sqrt{\psi_0}$ becomes

$$f(x;a) = x\, e^{-\frac{x^2+a^2}{2}} I_0\{ax\}$$

This is the distribution of a sine wave of amplitude P in Gaussian noise of mean square value ψ_0. The parameter "a" has the characteristics, therefore, of a signal to noise ratio. We see from the above substitutions that the shape of the distribution is determined entirely by the parameter "a". Two distributions with the same "a" will differ only by a scale factor.

Since the f(x;a) family of curves represents a set of possible distributions for the return voltages, a procedure was set up to test whether or not the returns did fit members of the family. This procedure is described in detail in AER-5A, Section VII, but will be condensed and repeated here.

It was decided that the decision as to whether or not an empirical distribution was of the form f(x;a) would be made on the basis of a comparison of the cumulative curves. However, rather than compare the empirical curve to $F(x;a) = \int_0^x f(t;a)\,dt$ for a number of values of "a", we obtained a statistic which was selective so far as possible values of "a" were concerned. That is, this statistic would tell us which F(x;a) our empirical curve should compare to if it were to compare to any.

For the W(R) distribution $E(R^2) = 2\psi_0 + P^2$

and $1/n \sum R_i^2 = \overline{R^2}$ is the maximum likelihood estimator of $E(R^2)$.

[redacted]

UNCLASSIFIED

[redacted]

UNCLASSIFIED

Now $$\int_0^{\sqrt{\psi_0 + \frac{P^2}{2}}} R/\psi_0 \, e^{-\frac{R^2+P^2}{2\psi_0}} \, I_0\{RP/\psi_0\} \, dR$$

$$= \int_0^{\sqrt{1+a^2/2}} x \, e^{-\frac{x^2+a^2}{2}} \, I_0\{ax\} \, dx$$

and the value of this integral is the function of "a" which is tabulated below.

a	$\int_0^{\sqrt{1+a^2/2}} x \, e^{-\frac{x^2+a^2}{2}} \, I_0\{ax\} \, dx$
0	.38
1	[illegible]
2	.15
3	[illegible]
4	[illegible]
5	[illegible]

[redacted]

UNCLASSIFIED

[redacted]

UNCLASSIFIED

Since $\overline{R^2}$ estimates $2\psi_0 + P^2$, $\sqrt{\overline{R^2}/2}$, will estimate $\sqrt{\psi_0 + P^2/2}$

and if the empirical cumulative density is of the form $F(x;a)$, its value at $\sqrt{\overline{R^2}/2}$ should compare to one of the values above. If it does we can proceed to make a direct comparison of the cumulative curves.

Confidence intervals are placed upon the estimator $\sqrt{\overline{R^2}/2}$ (See Section XVI), and this uncertainty is combined with the uncertainty connected with the estimated points to give confidence limits on the value of the empirical cumulative distribution at $E(\hat{R}^2)$. If these confidence limits enclose one of the values listed in the second column above, we make the comparison. If the confidence interval falls between two values, the comparison is made with both.

This method of elimination and then comparison was employed in the analysis of films 2-6, 2-7, and 2-21. At this time it was decided that to facilitate future comparisons with other families of curves the cumulative curves would all be plotted so that their 50% points fell ten centimeters out on the horizontal axis, and the comparisons would be made by means of overlays. The original statistic was retained, however, and its validity was confirmed by the purely visual tests which followed (Films 2-13, 2-5, 2-16, 2-10).

[redacted]

UNCLASSIFIED

[redacted]

UNCLASSIFIED

XVI. THE ESTABLISHMENT OF CONFIDENCE INTERVALS FOR THE ESTIMATION OF P_r AND $\sqrt{E(R^2)/2}$

In the individual film reports, confidence intervals are quoted on the estimations of the average return power, P_r, and the quantity $\sqrt{E(R^2)/2}$ where R is the return voltage. The estimators of both these quantities are functions of $\overline{R^2}$, $\hat{P}_r$ being $k\,\overline{R^2}$, and $\widehat{\sqrt{E(R^2)/2}}$ being $\sqrt{\overline{R^2}/2}$*. Consequently, we will first describe the method used to determine the confidence interval for $\overline{R^2}$ and then derive the others from it.

In the computation scheme that we use, our samples are broken up into groups of twenty each. It is this division that we utilize to obtain confidence limits on $\overline{R^2}$. From each twenty samples we obtain an estimate $\overline{R_i^2} = 1/20 \sum R^2$. These estimates are approximately normally distributed because of their character as means (central limit theorem). The standard deviation of their distribution is estimated by

$$\hat{\sigma} = \sqrt{\overline{A^2} - \overline{A}^2}$$

where $A_i = \overline{R_i^2}$, $\bar{A} = 1/n' \sum A_i$

and $\overline{A^2} = 1/n' \sum A_i^2$

Here n' is the number of groups of twenty samples in the total sample. If the total sample size exceeds [illegible], it will be 12. If the distribution of $\overline{R_i^2}$ has a standard deviation of $\hat{\sigma}$, then the distribution of $\overline{R^2}$ has a standard deviation of $\hat{\sigma}/\sqrt{n'}$, since

$$\overline{R^2} = 1/n' \sum \overline{R_i^2}.$$

*The estimator of a quantity g will be indicated by $\hat{g}$.

[redacted]

UNCLASSIFIED

[redacted]

UNCLASSIFIED

Hence $\pm 1.96\ \hat{\sigma}/\sqrt{n'}$ gives a 95% confidence interval for $\overline{R^2}$ as an estimate of the average of the voltage squared. The above is not in significant error because of the use of $\hat{\sigma}$ as an approximation to σ. For the values of n' which we used, the factor based on the "t" distribution did not differ appreciably from 1.96.

Since $P_r = k\,\overline{R^2}$, a 95% confidence interval for P_r is $\pm 1.96\ k\hat{\sigma}/\sqrt{m'}$. This interval is the one quoted for P_r in the individual film reports.

If

$$-\frac{1.96\,\hat{\sigma}}{\sqrt{n'}} < E(R^2) - \overline{R^2} < \frac{1.96\,\hat{\sigma}}{\sqrt{n'}}$$

then, assuming $\overline{R^2} > \dfrac{1.96\,\hat{\sigma}}{\sqrt{n'}}$,

$$\sqrt{\overline{R^2}/2 - \frac{1.96\,\hat{\sigma}}{2\sqrt{n'}}} < \sqrt{E(R^2)/2} < \sqrt{\overline{R^2}/2 + \frac{1.96\,\hat{\sigma}}{2\sqrt{n'}}}$$

Subtracting $\sqrt{\overline{R^2}/2}$ from both sides we have

$$\sqrt{\overline{R^2}/2 - \frac{1.96\,\hat{\sigma}}{2\sqrt{n'}}} - \sqrt{\overline{R^2}/2} < \sqrt{\frac{E(R^2)}{2}} - \sqrt{\overline{R^2}/2} < \sqrt{\overline{R^2}/2 + \frac{1.96\,\hat{\sigma}}{2\sqrt{n'}}} - \sqrt{\overline{R^2}/2}$$

Now

$$\left|\sqrt{\overline{R^2}/2 - \frac{1.96\,\hat{\sigma}}{2\sqrt{n'}}} - \sqrt{\overline{R^2}/2}\right| > \left|\sqrt{\overline{R^2}/2 + \frac{1.96\,\hat{\sigma}}{2\sqrt{n'}}} - \sqrt{\overline{R^2}/2}\right|$$

so a 95% confidence interval for $\sqrt{\overline{R^2}/2}$ as an estimator of $\sqrt{E(R^2)/2}$ given by

$$\pm\left\{\sqrt{\overline{R^2}/2} - \sqrt{\overline{R^2}/2 - \frac{1.96\,\hat{\sigma}}{2\sqrt{n'}}}\right\}$$

This is the confidence interval that is quoted in the individual film reports.

[redacted]

UNCLASSIFIED

[redacted]

UNCLASSIFIED

XVII. THE ESTABLISHMENT OF CONFIDENCE INTERVALS FOR THE CUMULATIVE DENSITY POINTS

A large sample estimate of the parameter p of the binomial distribution is approximately normally distributed with mean p and the standard deviation $\sqrt{p(1-p)}/\sqrt{N'}$ where N' is the independent sample size (See AER-5A, AER-2). We cannot use this standard deviation directly to obtain a confidence interval, since our samples are not independent, and hence the actual sample size cannot be used as an independent sample size. What we did was to determine an independent sample size equivalent to the actual non-independent sample size and use this equivalent in the formula above for the standard deviation.

This equivalent independent sample size was determined using a method which parallels that used to determine the confidence interval for $\bar{R}^2$. We estimate the probability p that a value is less than or equal to some level, e, using the estimator $\hat{p} = n/N$ where n is the number of values less than or equal to e, and N is the total number of samples. The $\hat{p}$ can be thought of as the average of a group of $\hat{p}_i$, estimates taken from successive groups of 20 samples each. In this case $\hat{p}_i = n_i/20$ where n_i is the number less than or equal to e in the 20 samples. These $\hat{p}_i$ are approximately normally distributed and their standard deviation is estimated by

$$\sigma_{\hat{p}_i} = \sqrt{\overline{\hat{p}_i^2} - \bar{p}_i^2}.$$

Since $\hat{p} = 1/n' \sum \hat{p}_i$, $\sigma_{\hat{p}_i}/\sqrt{n'}$ estimates the standard deviation of the distribution of $\hat{p}$. This empirical standard deviation is equated to the standard deviation expressed as a function of the independent sample size and the equation below is solved for N',

$$\sigma_{\hat{p}_i}/\sqrt{n'} = \frac{\sqrt{\hat{p}(1-\hat{p})}}{\sqrt{N'}}.$$

[redacted]

UNCLASSIFIED

[redacted]

UNCLASSIFIED

The estimator $\hat{p}$ is substituted for p and a value of $\hat{p}$ is chosen where the function $\sqrt{\hat{p}(1-\hat{p})}$ does not vary rapidly. This means that N' independent samples would yeild an estimate with the same confidence limits as the N actual samples did. Our N samples are equivalent then to N' independent samples in terms of the accuracy of the estimates.

For Zone 1 in each film we pick a $\hat{p}$ near the 50% level (since $\sqrt{p(1-p)}$ varies least here) and perform the above to obtain N'. This number N' is then used to obtain the 95% confidence limits for the cumulative density points. These limits are

$$\pm 1.96 \frac{\sqrt{\hat{p}(1-\hat{p})}}{\sqrt{N'}}$$

and are indicated with the plotting of the points.

Occasionally, where two different sampling procedures had been used, the samples were broken into two sets. In combining the estimates from these two sets the equivalent independent sample sizes were used as weights rather than the actual sample sizes. In this way the most accurate combined estimate was made.

[redacted]

UNCLASSIFIED

XVIII. DETERMINATION OF THE SCATTERING COEFFICIENT

The equation relating the scattering coefficient to the other radar parameters is

$$P_r = \int_A \frac{P_t \, K(\theta) \, G \, A_{eff}}{16\pi^2 \, R^4} \, dA$$

where P_r is the average return power, P_t is the transmitted power, R is the range, $K(\theta)$ is the scattering coefficient, G is the gain relative to a point source, θ is the angle of incidence, and "A_{eff}" is the effective area of the antenna. This is an integral over the target area and may be written

$$P_r = \int_0^{2\pi} \int_{R_1}^{R_2} \frac{P_t \, K(\theta) \, G(\theta, \phi) \, A_{eff}(\theta, \phi)}{16\pi^2 \, R^4} \, \rho \, d\rho \, d\phi$$

The orientation of these angles may be seen from the diagram below.

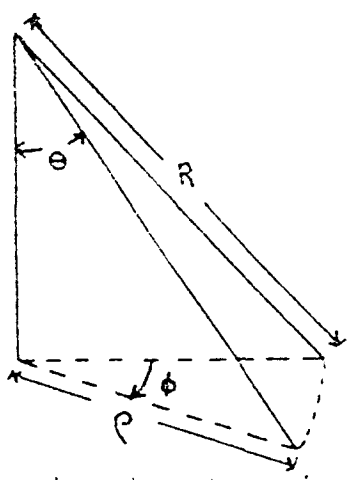

We are assuming that the antenna is directed vertically so the angle θ is also the angle between the antenna axis and the direction to the element of area.

In simplifying the relationship we first assume that G and A_{eff} are independent of ϕ (i.e., that the antenna is circularly symmetric). We can then integrate ϕ out, getting

$$P_r = \frac{2\pi}{16\pi^2} \int_{R_1}^{R_2} \frac{P_t \, K(\theta) \, G(\theta) \, A_{eff}(\theta)}{R^4} \, \rho \, d\rho$$

[redacted]

UNCLASSIFIED

Next, we assume that P_t is constant and that $A_{eff} = \frac{G\lambda^2}{4\pi}$

This yields

$$P_r = \frac{\lambda^2 P_t}{32\pi^2} \int_{\Lambda_1}^{\Lambda_2} \frac{G^2(\theta)\ K(\theta)}{R^4}\ \rho\, d\rho$$

Since the angular intervals over which we are integrating are quite small, we treat $K(\theta)$ as a constant with regard to the limits of the integral. This we give as an average $K(\theta)$ for the angular interval. Hence

$$P_r = \frac{P_t \lambda^2}{32\pi^2} K(\theta) \int_{\Lambda_1}^{\Lambda_2} \frac{G^2(\theta)}{R^4}\ \rho\, d\rho$$

The antenna gain was determined as follows. The power P_θ per unit solid angle at an angle θ was found to be approximately

$$P_\theta = P_o \cos 3\theta \qquad 0 \leq \theta \leq 30^\circ$$

$$P_\theta = 0 \qquad \text{otherwise}$$

where P_o is the maximum power per unit solid angle. The gain is given by the following equation:

$$G = P_\theta / P_{pt.\ source}$$

where $P_{pt\ source}$ is the power per unit solid angle that would be generated by a point source with the same total transmitted power.

[redacted]

UNCLASSIFIED

[redacted]

UNCLASSIFIED

Hence

$$G = \frac{4\pi P_\theta}{P_t} = \frac{4\pi P_o \cos 3\theta}{P_o \int_\Omega \cos 3\theta \sin\theta \, d\theta \, d\phi}$$

where P_t is the total transmitted power. Cancelling and evaluating,

$$\left[0 \leq \phi < 2\pi, \; 0 \leq \theta \leq \pi/6\right]$$

yields $G = 32 \cos 3\theta$.

This reduces our equation further to

$$P_r = \frac{32 P_t \lambda^2 K(\theta)}{\pi^2} \int_{\Omega_1}^{\Omega_2} \frac{\cos^2 3\theta}{R^4} \rho \, d\rho$$

Solving for $K(\theta)$ we have

$$K(\theta) = \frac{\pi^2}{32 P_t \lambda^2} \times \frac{P_r}{\int_{\Omega_1}^{\Omega_2} \frac{\cos^2 3\theta}{R^4} \rho \, d\rho}$$

This is the formula used in calculating the $K(\theta)$ for the individual film reports.

[redacted]

UNCLASSIFIED

FLIGHT SERIES TWO — FL

Film No. (C. F. [illegible] No.)	1	[illegible]	[illegible]	[illegible]	5	[illegible]	[illegible]	[illegible]	[illegible]	[illegible]	[illegible]
Grid Film Format	R	R	R	R	W	W	W	W	W	W	W
Date No.	[illegible]	[illegible]	8	8	8	[illegible]	[illegible]	8	[illegible]	[illegible]	[illegible]
Single Station	[illegible]	[illegible]	2 x 1	[illegible]	[illegible]	[illegible]	1 x 1	[illegible]	1 x 1	[illegible]	[illegible]
Autopilot (volts) Orientation (degrees)	16.2 0	11.0 [illegible]	[illegible] 40	[illegible]	16.0 0	[illegible] 40	16 0	[illegible] [illegible]	[illegible]	[illegible]	[illegible]
Altitude (feet) at IGC	—	—	—	—	[illegible]	8200	[illegible]	[illegible]	[illegible]	[illegible]	[illegible]
Power Plant [illegible]	[illegible]	[illegible]	[illegible]	[illegible]	160	[illegible]	[illegible]	—	[illegible]	—	[illegible]
Run Gen. Attitude Motion [illegible]	[illegible]	[illegible]	[illegible]	[illegible]	[illegible]	[illegible]	[illegible]	[illegible]	[illegible]	[illegible]	[illegible]
[illegible] Supply Voltage	[illegible]	[illegible]	[illegible]	[illegible]	[illegible]	[illegible]	[illegible]	[illegible]	[illegible]	[illegible]	[illegible]
Air Speed (mph)	[illegible]	[illegible]	[illegible]	[illegible]	[illegible]	[illegible]	[illegible]	[illegible]	180		[illegible]
Temp. (°F)	[illegible]	[illegible]	[illegible]	[illegible]	[illegible]	[illegible]	[illegible]	[illegible]	[illegible]	[illegible]	[illegible]
Pressure Altitude (ft)	[illegible]	[illegible]	[illegible]	[illegible]	[illegible]	[illegible]	[illegible]	[illegible]	[illegible]	[illegible]	[illegible]
Notes			A.F								

—FLIGHT LOG

11	12	13	14	15	16	17	18	19	20	21	22	23
U	U	U	U	✓ U	✓ U	U	R	U	U	✓ U	✓ U	✓ U
[illegible]	[illegible]	[illegible]	6	2	6	2	6	2	6	6	2	[illegible]
1 x [illegible]	2 x 2	2 x 4	2 x 4	2 x 8	2 x 8	2 x 4	2 x 4	2 x 4	[illegible] x 4	[illegible]	[illegible]	[illegible]
16 0	[illegible]	16 0	16 0	16 0	16 0	9 30	9 30	9 30	9 30	16 0	16 0	[illegible]
[illegible]	[illegible]	[illegible]	10840	11105	11110	11280	—	8045	8020	8065	[illegible]	[illegible]
—	—	[illegible]	[illegible]	[illegible]	[illegible]	[illegible]	[illegible]	[illegible]	[illegible]	[illegible]	[illegible]	[illegible]
[illegible]	[illegible]	[illegible]	[illegible]	55	57	[illegible]	54	57	[illegible]	47	[illegible]	[illegible]
[illegible]	[illegible]	[illegible]	[illegible]	[illegible]	[illegible]	[illegible]	[illegible]	[illegible]	[illegible]	[illegible]	[illegible]	[illegible]
[illegible]	[illegible]	[illegible]	[illegible]	[illegible]	[illegible]	[illegible]	?	?	?	[illegible]	[illegible]	[illegible]
[illegible]	[illegible]	[illegible]	[illegible]	[illegible]	[illegible]	[illegible]	[illegible]	[illegible]	[illegible]	[illegible]	[illegible]	[illegible]
[illegible]	[illegible]	[illegible]	[illegible]	11855	[illegible]	[illegible]	[illegible]	9100	9100	[illegible]	[illegible]	[illegible]
	[illegible]	[illegible]	[illegible]		[illegible]		[illegible]	[illegible]	[illegible]	[illegible]	[illegible]	

NOTES:

GB Correlation: [illegible]

Signal Generator Freq[illegible]

Ground Speeds: none [illegible]

Radar Altitudes: none

Scope Input Attenuat[illegible]

Scope Intensity: Full

Note A: Very weak [illegible]

Note B: [illegible]

Note C: [illegible]

Note D: [illegible]

Note E: [illegible]

Note F: [illegible]

Note G: [illegible]

Note H: [illegible]

Note I: [illegible]

Note J: [illegible]

Note K: [illegible]

FIGUR[illegible]

[redacted]

UNCLASSIFIED

9	20	21	[illegible]	[illegible]
U	U	✓ U	✓ U	✓ U
2	6	6	2	6
x 4	2 x 4	1 x 1	1 x [illegible]	1 x 1
9 30	9 30	16 0	16 0	[illegible] 0
[illegible]	[illegible]	2065	[illegible]	[illegible]
168	[illegible]	[illegible]	[illegible]	[illegible]
57	[illegible]	47	[illegible]	[illegible]
[illegible]	[illegible]	[illegible]	[illegible]	[illegible]
[illegible]	[illegible]	[illegible]	[illegible]	[illegible]
[illegible]	[illegible]	[illegible]	[illegible]	[illegible]
[illegible]	9100	[illegible]	[illegible]	[illegible]
[illegible]	[illegible]	[illegible]	[illegible]	

NOTES:

GR Correlation: 1 (i.e., GR film run associated with first K-17 photo in series — whether before or after and how long is not definitely known.)

Signal Generator Frequency: [illegible] mc/s for all runs.

Ground Speeds: none available.

Radar Altitudes: none available.

Scope Input Attenuation: vernier [illegible] for all runs.

Scope Intensity: Full, for all runs.

Note A: Very weak signal

Note B: K-17 photos for 2 extra runs [illegible]

Note C: Signal close to saturation

Note D: [illegible]

Note E: [illegible] transmitter pulse [illegible]

Note F: [illegible] reel [illegible] DBM.

Note G: [illegible] start of reel at [illegible] DBM

Note H: [illegible] start of reel at [illegible] DBM

Note I: [illegible] start of reel at [illegible] DBM

Note J: [illegible] pulse and theater missing [illegible] at [illegible] DBM [illegible] order from start of film.

Note K: [illegible] pulse [illegible] at [illegible] DBM

Note L: [illegible] start of film.

Note M: No transmitted pulse picture.

FIGURE 1

UNCLASSIFIED

[redacted]

UNCLASSIFIED

9	U-	8	1 x 1	OK	RL-400-110	0-100	64-84	Time markers fall in leading edges of return pulses; 5% anomalous traces.
10	U-	8	1 x 1	OK	RL-400-75	20-168	80-92	Time markers fall in center of return pulses.
11	U-	8	1 x 2	OK	RL-405-73	0-60	60-64	Time marker falls in return pulses just after peak.
12	U-	8	2 x 8	OK	LR-370-107	0-64	40-48 irregular tops	Time markers split return pulses.
13	U	2	2 x 4	OK, except high noise	LR-385-98	0-44	36-48	10% anomalous traces.
14	U-	6	2 x 4	OK	LR-375-95	0-68	56-68	Marker falls in middle of return pulses; 4% anomalous traces.
15	U-	2	2 x 8	OK	LR-385-105	0-60	32-40 irregular tops	Marker falls in rise of return pulse; knocks out peak.
16	U-	6	2 x 8	OK	LR-385-110	0-76	28-44	Marker falls in rise; peak usually readable.
17	U	2	2 x 4	OK	LR-375-95	0-80	14-40	6% anomalous traces
18	R	6	2 x 4	OK	LR-395-100	0-80	24-60	Return not bracketed by time marker; 8% anomalous
19	U-	2	2 x 4	OK	LR-390-100	0-80	56-80	Time marker falls in rise of return pulses; impossible to read peak values. 11% anomalous.
20	U	6	2 x 4	OK	LR-390-110	0-80	16-32	20% anomalous
21	U	6	1 x 1	OK	RL-390-95	0-112	70-80	
23	U	6	1 x 1	OK	RL-390-100	0-160	48-64	
22	U	2	1 x 1	OK	RL-375-100	0-112	76-84	Under 1% anomalous

FIGURE 2

UNCLASSIFIED

UNCLASSIFIED

UNCLASSIFIED

RESULTS OF SURVEY OF SERIES 2 FILMS

FILM NO.	FILM RATING	SITE NO.	SCOPE SET-TING	CONTRAST-TRACE-NOISE	SWEEP DIRECTION-TRACE LENGTH-MARKER INTERVAL	RETURN RANGE	COMPARATOR RANGE	COMMENTS
1	Reject	8	2 x 8	OK	LR-375 mm-?	0-84	56-64	Return not bracketed by time markers.
2	R	8	2 x 8	OK	LR-375-?	0-48	40-68	Return not bracketed by time markers.
3	R	8	2 x 1	OK	LR-375-?	0-24 mostly zero	32-56, very irregular	Return not bracketed by time markers; comparator cannot be read with reproducibility.
4	R	8	2 x 8	Poor contrast, faint trace	RL-370-115	0-64	56-72	Photography very poor; almost impossible to read. Trace reversed from others of same scope setting.
5	Usable	8	1 x 1	OK	RL-400-110	0-84	approx. 84	
6	U	8	2 x 1	OK	LR-405-104	0-24	very irregular	Comparator cannot be read with good reproducibility.
7	U	8	1 x 1	OK	RL-400-70	0-92	74-90	
8	U	8	2 x 8	OK	LR-395-112	0-24 mostly very low	16-28 irregular tops	
9	U-	8	1 x 1	OK	RL-400-110	0-100	64-84	Time markers fall in leading edges of return pulses; 4% anomalous traces.
10	U-	8	1 x 1	OK	RL-400-75	20-168	80-92	Time markers fall in center of return pulses.
11	U-	8	1 x 2	OK	RL-405-73	0-60	60-64	Time marker falls in return pulses just

FIGURE 2

001756

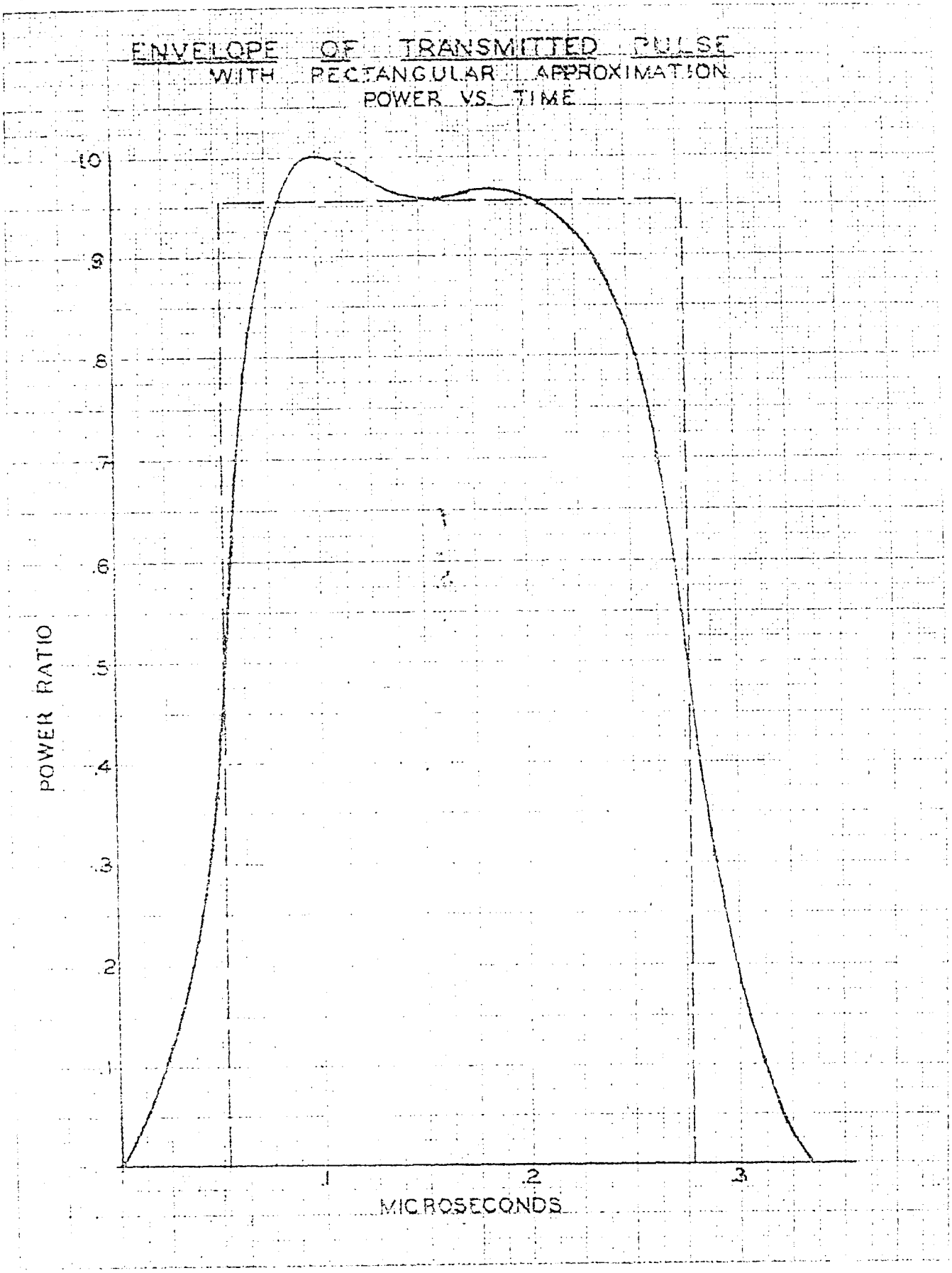

FIGURE 3 [redacted]

UNCLASSIFIED

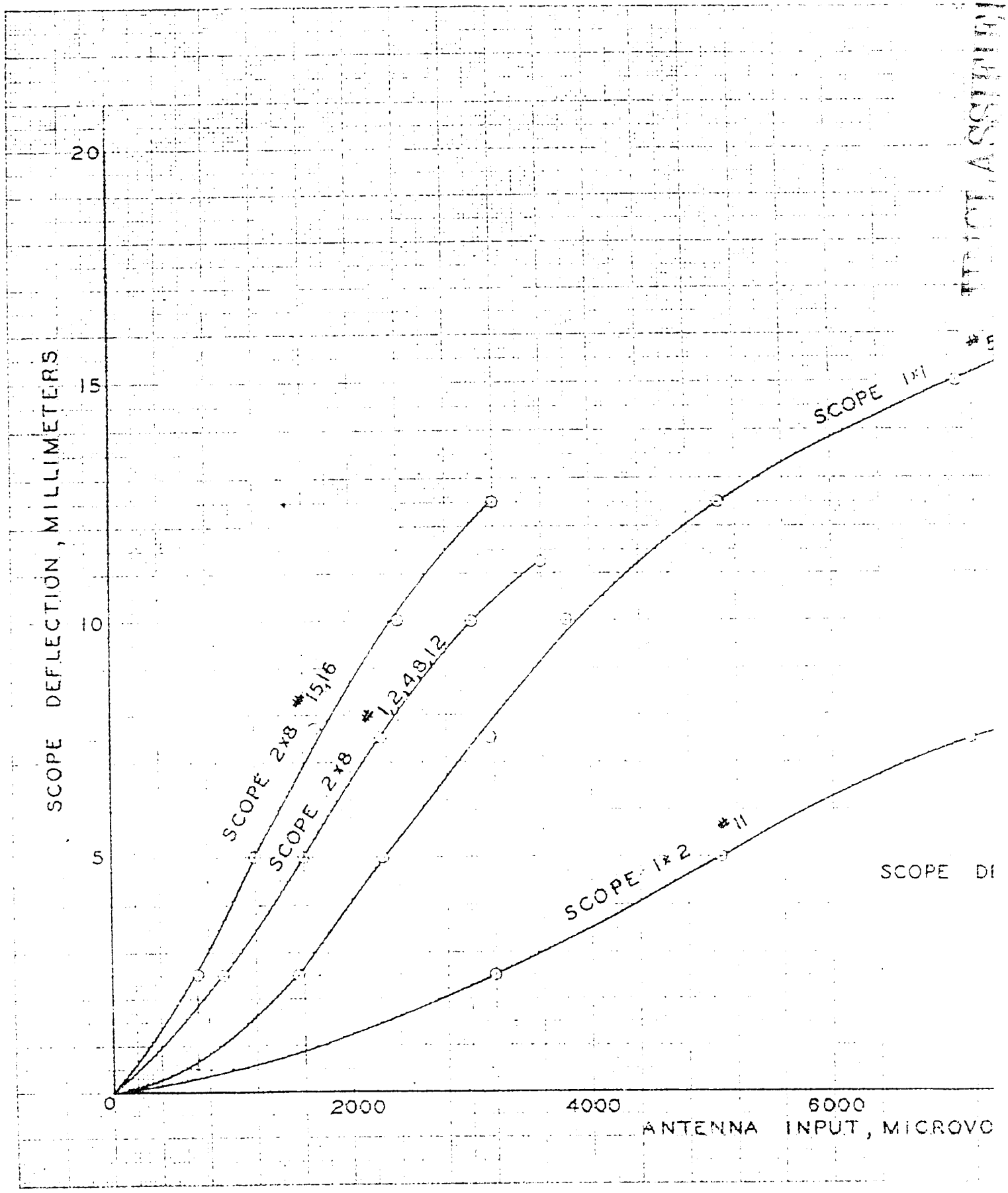

UNCLASSIFIED

[redacted]

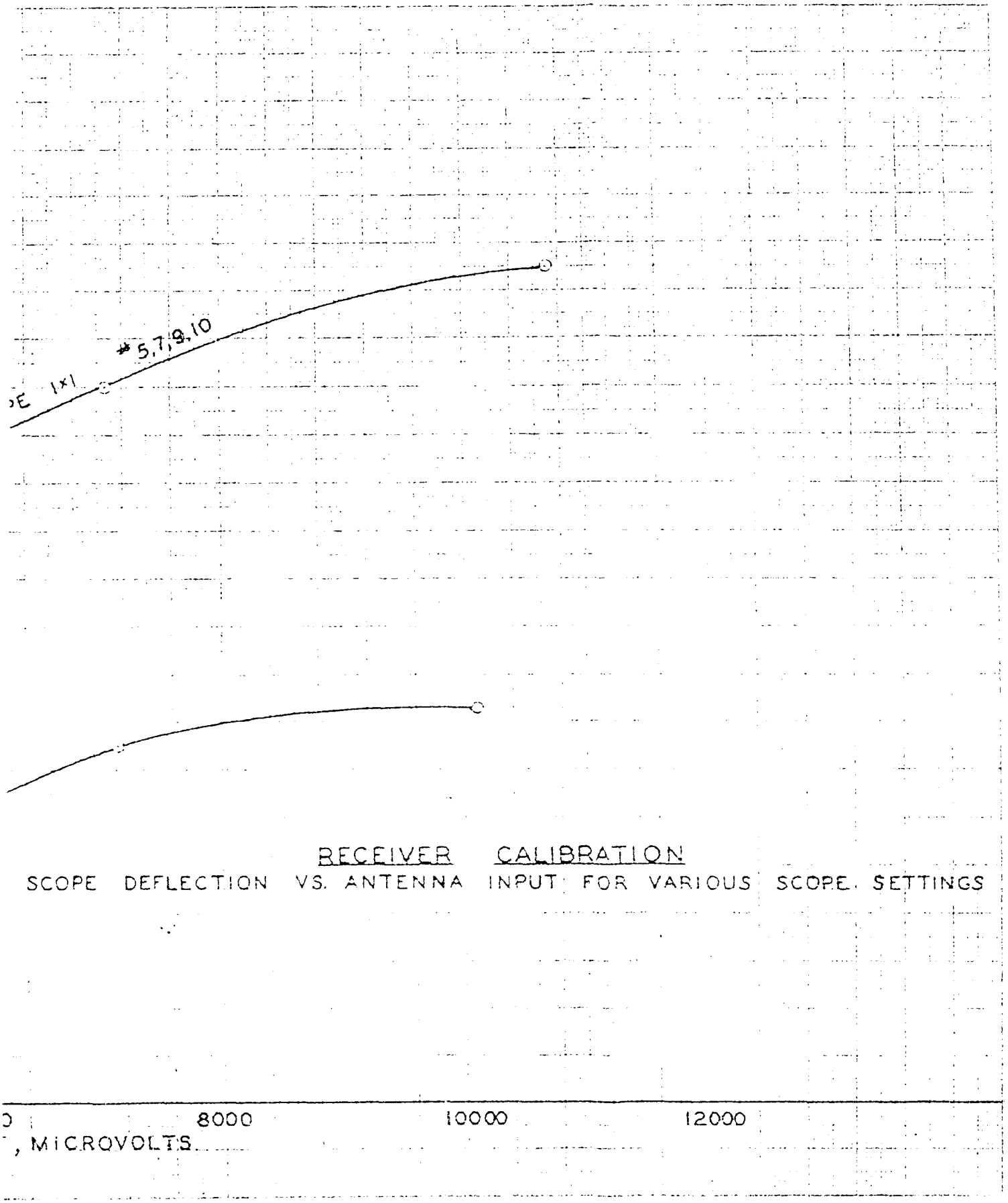

RECEIVER CALIBRATION

SCOPE DEFLECTION VS. ANTENNA INPUT FOR VARIOUS SCOPE SETTINGS

FIGURE 4 [redacted]

UNCLASSIFIED

UNCLASSIFIED

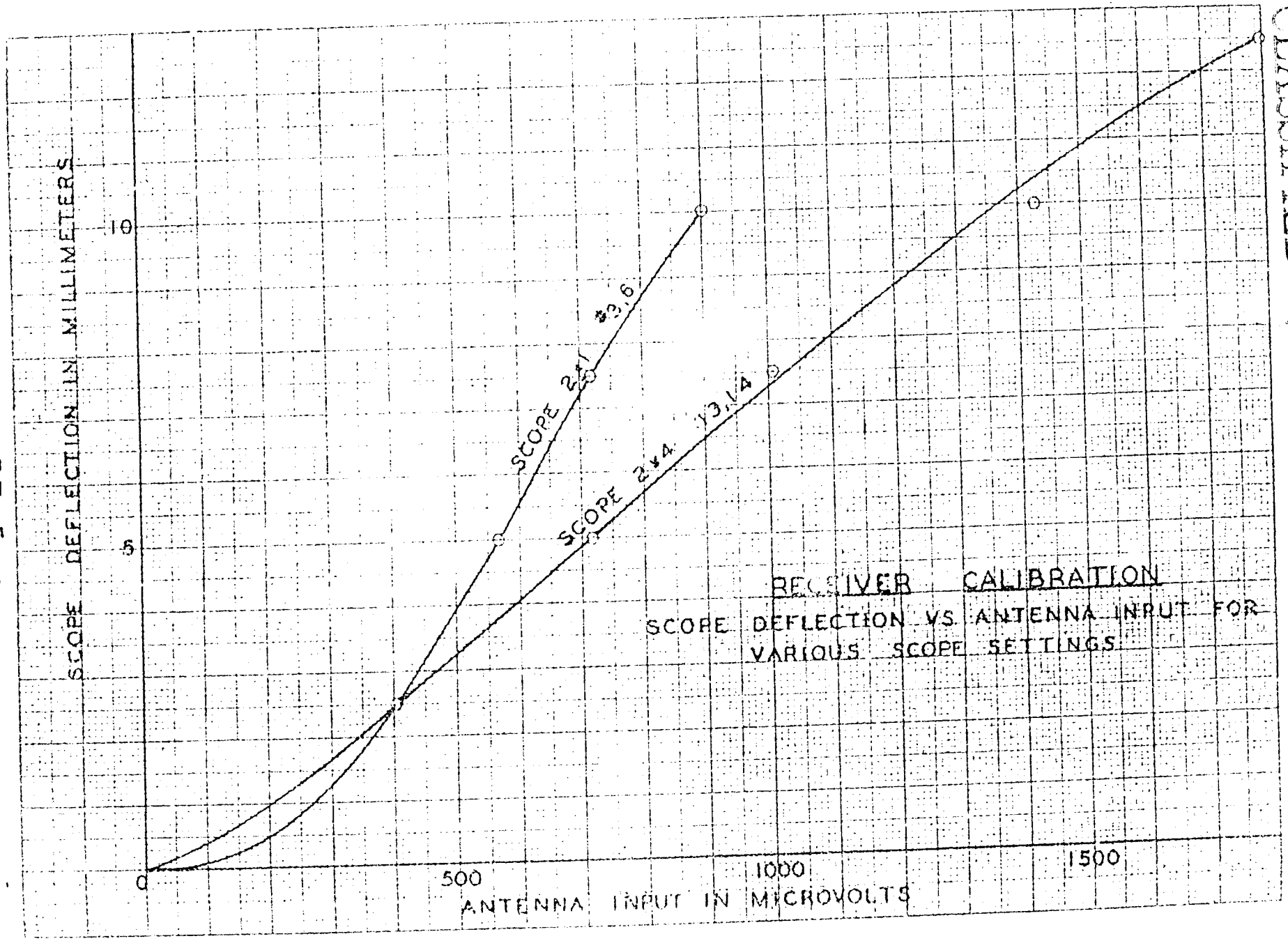

FIGURE 5

UNCLASSIFIED

001769

001760

[redacted]

UNCLASSIFIED

This report represents the group effort of Ivan L. Carbine, E. Lynn Cleveland, and Peter D. Welch.

E. L. Cleveland by P.W.
E. Lynn Cleveland

Approved:

Ralph Dressel
Ralph A. Dressel
Supervisor

George A. Gardner
Director

[redacted]

UNCLASSIFIED